Physics of the Solid State, 2023, Vol. 65, No. 4

06,13

Formation and study of metal-insulator-semiconductor structures based on hafnium oxide films

© *M.S. Afanasiev, D.A. Belorusov, D.A. Kiselev, V.A. Luzanov, G.V. Chucheva*¶

Fryazino Branch, Kotel'nikov Institute of Radio Engineering and Electronics, Russian Academy of Sciences, Fryazino, Moscow oblast, Russia

¶ E-mail: gvc@ms.ire.rssi.ru

Received December 18, 2022
Revised December 18, 2022
Accepted January 24, 2023

Films of hafnium oxide (HfO_2) were synthesized on a silicon substrate by magnetron sputtering of a target with a similar composition. The results of studies of the structural composition of HfO_2 films and the electrical properties of metal-insulator-semiconductor (Ni-HfO_2-*n*-Si) structures are presented

Keywords: Metal−dielectric−semiconductor (MDS) structures, hafnium oxide (HfO_2) ferroelectric films, piezoelectric response, microstructure, electrical properties.

DOI: 10.21883/PSS.2023.04.55995.8

1. Introduction

Flash-memory is the leader in the market of nonvolatile memory devices as of today, however, its use is limited by relatively slow operating speed and low number of possible switching operations [1]. In contrast to flash-memory, ferroelectric-based memory devices have potentially unlimited operational life and high speed of read and write operations [2,3]. Today, the only commercially available ferroelectric memory devices are random access FRAM with the following ferroelectric types used as the functional layer: $Pb[Zr_xTi_{1-x}]O_3$, $SrBi_2Ta_2O_9$, $BiFeO_3$. They have a number of shortcomings related to the high sensitivity to interface and stoichiometry, as well as to the low displacement of the conduction band in relation to the Fermi level of silicon, which limits the possibility of development of a ferroelectric memory compatible with the modern silicon technology [4]. Also worth noting is the discovered absence of external field penetration into the semiconductor due to the screening provided by recharging of localized electron states at the $Ba_xSr_{1-x}TiO_3$/Si interface [5,6]. All these challenges result in a situation that writing density of these devices is far below than that of flash-memory and further development of ferroelectric memory is impossible without investigation of new materials [7], the most promising of which is hafnium oxide [8]. A wide range of hafnium compounds (oxynitrides, silicates, oxides) are so-called „high-k" materials, which are promising for the formation of the thin gate dielectric of MOS-transistors [9–11] that allows for simplifying to a significant extent the implementation of new memory devices in the existing technology stack of materials.

This study presents results of investigation of electrophysical properties of HfO_2 thin films synthesized on silicon substrates.

2. Samples and experiment procedure

Hafnium oxide (HfO_2) films are formed on *n*-type silicon substrates (100) by high-frequency magnetron sputtering of a ceramic target with similar composition in the mixture of argon and oxygen in the ratio of 10 : 1 at a total pressure in the chamber of 0.4 Pa. The gas discharge power density was 2 W/cm^2. The deposition rate was about 200 nm/h. The radiation heating of the substrate in the process of sputtering provided sufficient surface mobility of the deposited particles to form the oxide.

Two identical metal−dielectric−semiconductor (MDS) structures were formed for the study: Si/HfO_2/Ni and Si/$HfO_{2(ann)}$/Ni. The difference between them is that the Si/$HfO_{2(ann)}$/Ni sample after the synthesis of HfO_2 film was subjected to thermal annealing in the oxygen atmosphere at a temperature of 500°C for 30 min.

The structure of produced films was studied by X-ray diffractometry using a DRON setup (Russia). Thickness of HfO_2 films and the presence of transition layers were determined by scanning electron microscopy (SEM) using a NovaNanoSem 230 microscope by FEI.

The topography of HfO_2 films, the polarization processes and the relaxation of signal of polarized areas were carried out using a Ntegra Prima scanning probe nanolaboratory (NT-MDT SI, Russia) in the piezoresponse force microscopy (PFM). Vertical component of the PFM signal (Mag×Cos channel) was recorded by applying alternating voltage with an amplitude of 5 V and a frequency of 20 kHz to the NSG10/TiN conductive probe (Tipsnano, Tallinn, Estonia). Loops of the residual piezoelectric hysteresis are obtained using a script for the Nova software. The time of direct voltage pulse supply and the time of piezoelectric response signal recording after removal of the voltage were 25 ms. The voltage varied from −10 to +10 V and in the return direction with a step of 0.1 V. 5 loops of

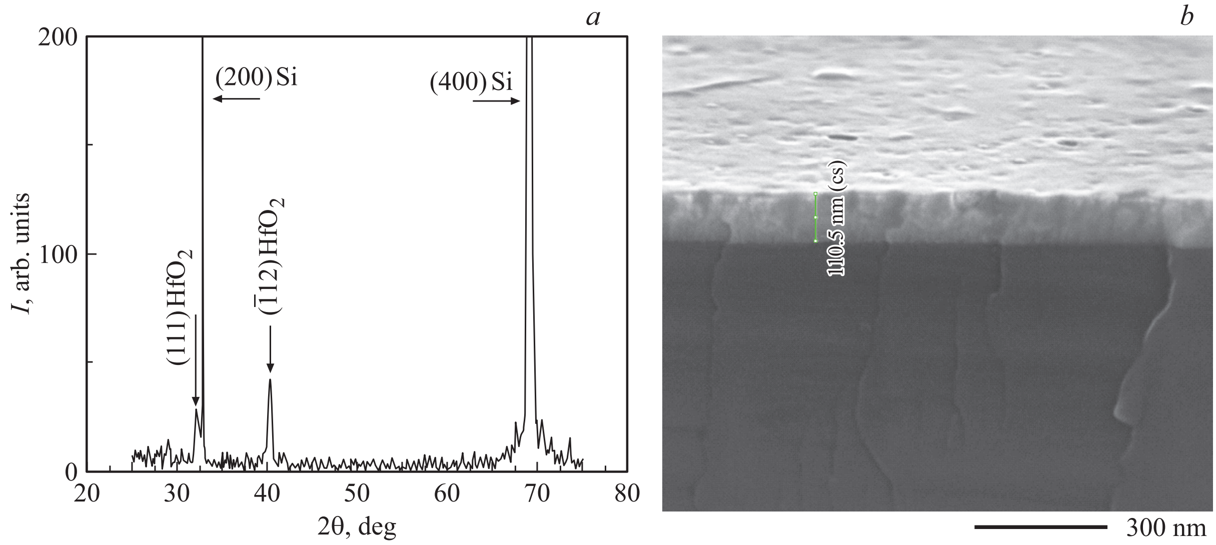

Figure 1. X-ray diffraction pattern (*a*) and SEM-image of the cleavage (*b*) of the Si/HfO_2/Ni structure.

hysteresis for each of three different locations of the films were obtained and averaged.

To investigate electrophysical properties of the produced HfO_2 films, MDS-structures of Ni-HfO_2-*n*-Si have been formed. The nickel electrode with an area of $2.7 \cdot 10^{-4}\,cm^2$ and a thickness of 150.0 ± 10 nm was applied by electron-beam sputtering through shadow mask. The temperature of the structure in the process of deposition was $70 \pm 5^\circ$C, the nickel deposition rate was 2.0 ± 0.2 Å/s.

Capacitance-voltage curves (CV-curves) of MDS-structures were measured by an automated experimental setup [12] using a LCR (Agilent) precision meter and a picoammeter by Keithley.

3. Results and discussion

3.1. Structural investigations of structures with hafnium oxide film

Fig. 1, *a, b* shows diffraction patterns and SEM-image of cleavage of the Si/HfO/Ni structure.

The diffraction pattern shows the presence of two peaks, which can be referred to (111) and $(\bar{1}12)$ reflections for the monoclinic phase of hafnium dioxide. However, a visible displacement of peaks is indicative of the presence of significant macrostresses in the formed layers.

SEM-image has shown that thickness of the HfO_2 film is 110 ± 5 nm and no transition layers in the structure. Diffraction pattern and SEM-image for the Si/$HfO_{(ann)}$/Ni structure had similar form.

Fig. 2 shows images of the surface of HfO_2 films under study recorded by scanning probe microscope (SPM). Root-mean-square roughness of the initial film surface was 0.4 nm with an average crystallite diameter of 32 nm (Fig. 2, *a*). The annealing of HfO_2 film results in an increase in the crystallite diameter up to 112 nm, at the same time the surface roughness increases Rms = 0.7 nm (Fig. 2, *b*).

3.2. Investigations of HfO_2 films by scanning probe microscopy methods

Fig. 3, *a, b* shows the result of direct voltage polarization of the hafnium oxide film surface by means of applying to the cantilever a positive (+8 V — „light“ left rectangle) and a negative (−8 V — „dark“ right rectangle) voltage: *a* — initial film, *b* — after annealing.

It can be seen from the profiles of piezoelectric response signal (Fig. 3, *c*) that signal of the region polarized by negative voltage is greater than that of regions polarized by positive voltage in relation to the initial piezoresponse signal for unpolarized region („zero level“), with this phenomenon being more evident for the initial film (Fig. 3, *c*, curve *1*). For the annealed HfO_2 film the intensities of signals for positive and negative regions become approximately the same (Fig. 3, *c*, curve *2*). In addition, conspicuous is the „blurring“ of boundaries of polarized regions of the HfO_2 film after annealing (polarized region in the initial film have a regular rectangular shape), which can be associated with the increased conductivity of grain boundaries.

Fig. 3, *d* shows residual loops of the piezoelectric hysteresis of hafnium oxide films that also confirm the effect of polarization switching at the nanoscale level. It has been found that annealing of the HfO_2 film results in increase in the piezoelectric response signal. However, no changes in the magnitude of the switching voltage were observed.

3.3. Electrophysical properties of Si/HfO_2/Ni and Si/$HfO_{2(ann)}$/Ni structures

Fig. 4, *a, b* shows CV-curves of Si/HfO_2/Ni and Si/$HfO_{2(ann)}$/Ni structures measured at room temperature at

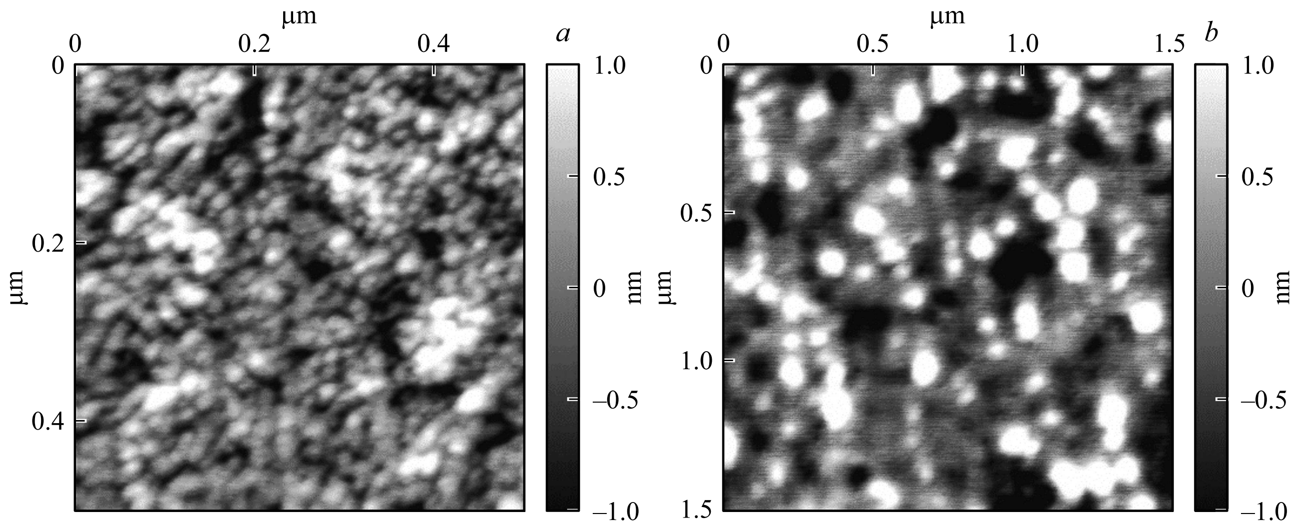

Figure 2. Topography image of the HfO_2 film surface: *a* initial film, *b* — film after annealing.

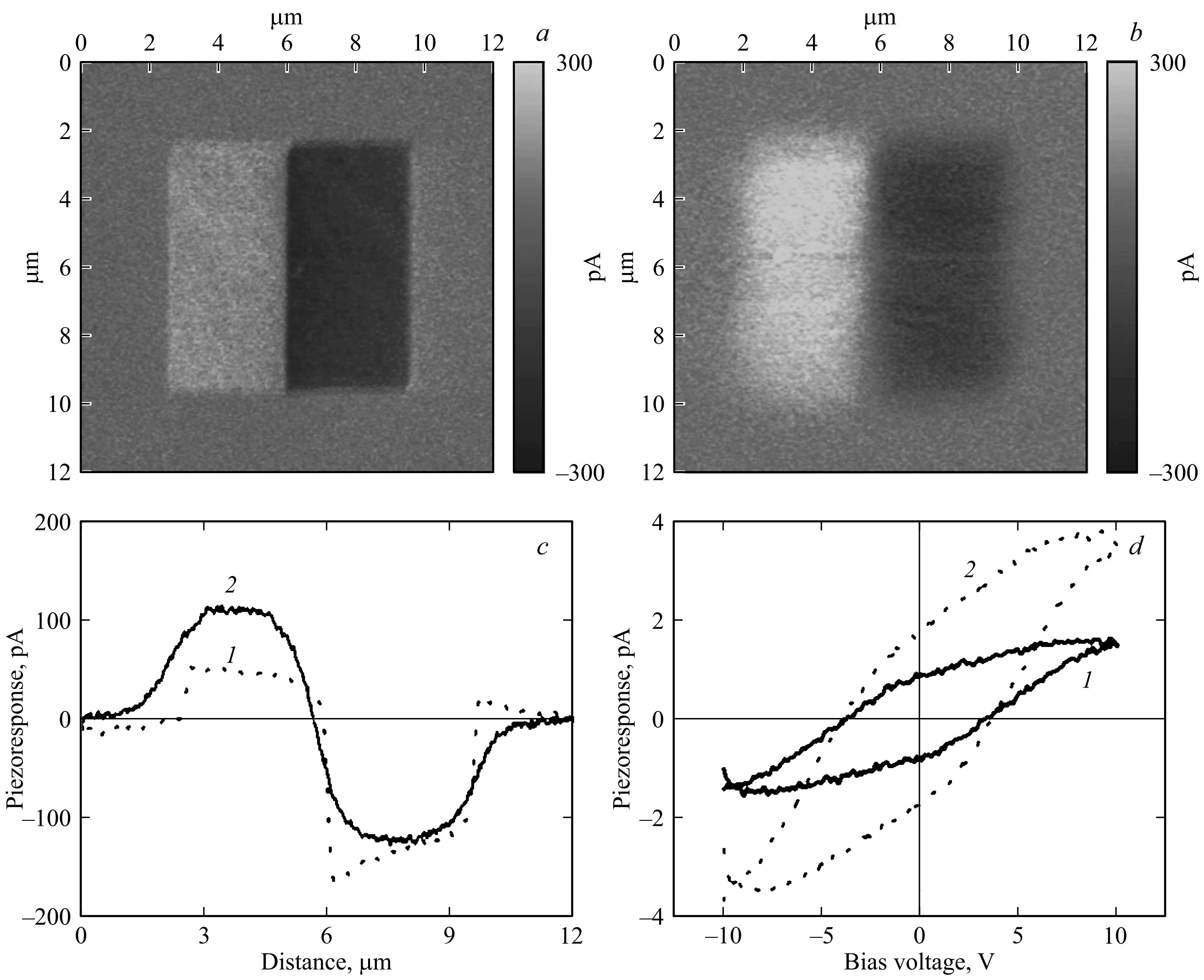

Figure 3. Piezoelectric response signal after polarization by direct voltage: +8 V — to the left semisquare and −8 V to the right semisquare; *a* — initial film, *b* — after annealing; *c* — profiles of piezoelectric response signal immediately after polarization; *d* — residual piezoelectric hysteresis loops. curve *1* — before annealing, curve *2* — after annealing.

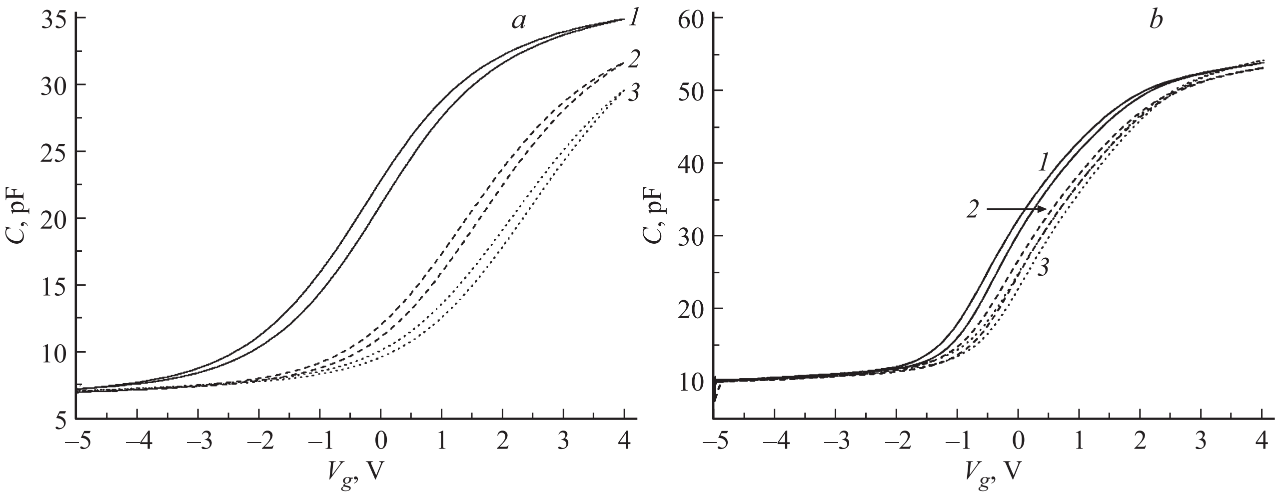

Figure 4. CV-curves of structures: *a* — Si/HfO_2/Ni, *b* — Si/$HfO_{2(ann)}$/Ni. Numbers of curves: *1* (solid thick line) — measurements at a frequency of 100 kHz, *2* (dashed line) — measurements at a frequency of 500 kHz, *3* (dotted line) — measurements at a frequency of 1000 kHz.

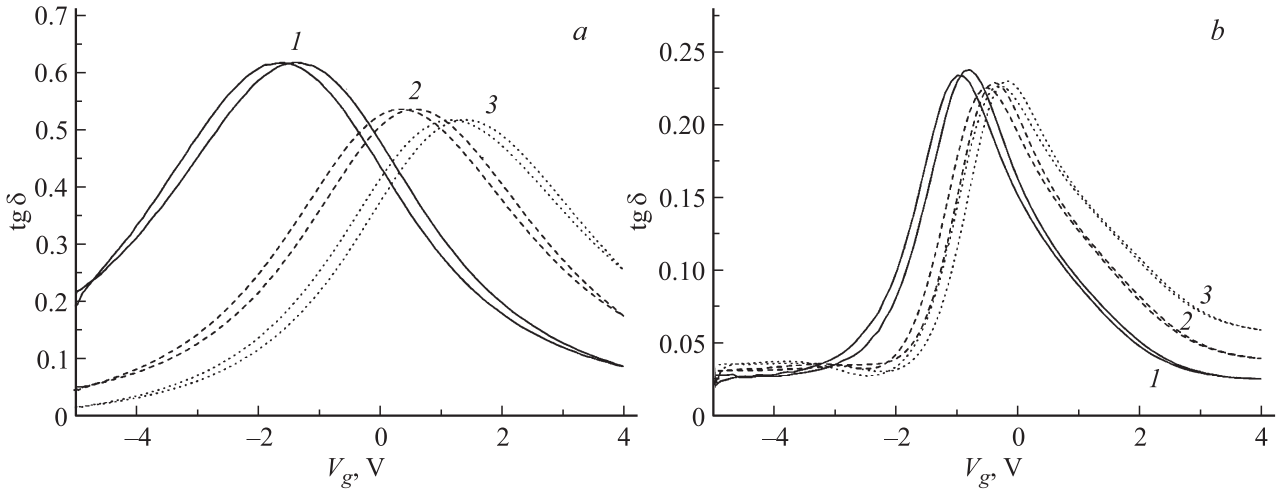

Figure 5. Dielectric loss tangent (tg δ) of MDS-structures as a function of voltage V_g; *a* — Si/HfO_2/Ni; *b* — Si/$HfO_{2(ann)}$/Ni. Numbers of curves: *1* (thick solid line) — measurements at a frequency of 100 kHz, *2* (dashed line) — measurements at a frequency of 500 kHz, *3* (dotted line) — measurements at a frequency of 1000 kHz.

frequencies of 100, 500 and 1000 kHz. The bias voltage V_g was applied to the samples varying from -5 to $+4$ V and in reverse direction with a step of 0.1 V.

The dependencies of structure capacitance on bias voltage have shapes of hysteresis loops. Measurements have shown that at a frequency of 100 kHz maximum capacitance ($C_{\max}$) of the Si/HfO_2/Ni structure is 35 pF, and that of the Si/$HfO_{2(ann)}$/Ni structures is 53 pF.

Also, it should be noted that the Si/$HfO_{2(ann)}$/Ni sample (Fig. 4, *b*) demonstrates a considerably less frequency shift of the CV-curve in relation to $V_g = 0$ V.

The analysis of CV-curves has shown that width of the hysteresis loop of the Si/$HfO_{2(ann)}$/Ni structure is less than that of the Si/HfO_2/Ni structure, however, both samples are characterized by equal loop widths at 500 kHz and 1000 kHz, and a wider loop at 100 kHz. Thus, width of the hysteresis loop of the Si/HfO_2/Ni sample at 100 kHz was about 0.25 V, width at 500 kHz and 1000 kHz was 0.23 V, and width of the hysteresis loop of the Si/$HfO_{2(ann)}$/Ni at 100 kHz was 0.15 V, and width at 500 kHz and 1000 kHz was 0.13 V. As a result of experimental data processing, the effective permittivity of the HfO_2 film has been determined: Si/HfO_2/Ni — 22; Si/$HfO_{2(ann)}$/Ni — 26.

Fig. 5, *a, b* shows dependencies of dielectric loss tangent (tg δ) on voltage V_g for Si/HfO_2/Ni and Si/$HfO_{2(ann)}$/Ni structures. Measurement modes are similar to those of CV-curve measurements.

The analysis of graphs has shown that maximum tg δ of the Si/$HfO_{2(ann)}$/Ni structure is less than that of the Si/HfO_2/Ni structure, and is 0.24 and 0.63, respectively.

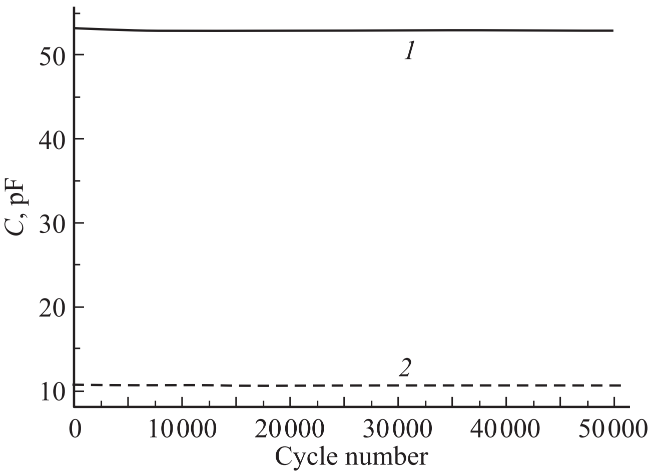

Figure 6. Maximum and minimum capacitance values of $Si/HfO_{2(ann)}/Ni$ structures depending on switching cycles. Numbers of curves: *1* (solid line) — measurements at a voltage of $+3.5$ V, *2* (dashed line) — measurements at a voltage of -3.5 V.

Fig. 6 shows maximum and minimum capacitance values of $Si/HfO_2/Ni$ and $Si/HfO_{2(ann)}/Ni$ structures depending on number of switching cycles. A voltage of $-3.5- +3.5$ V was applied to the structures by alternating the voltage for 0.5 s. 50000 cycles were carried out ($-3.5- +3.5$ V).

It has been found that after 50000 cycles of switching of the $Si/HfO_{2(ann)}/Ni$ structure the capacitance and the shape of curve have no changes.

The attempts to carry out such measurements for the $Si/HfO_2/Ni$ structure were unsuccessful because after about 2 cycles the structures demonstrated breakdown.

4. Conclusion

X-ray diffraction and topographic measurements have shown that HfO_2 films deposited by magnetron sputtering from a HfO_2 target have a stoichiometric composition and a monoclinic structure with a crystallite diameter of 32 nm. Methods of scanning probe microscopy after the local polarization have detected an asymmetry of the signal from regions with different direction of polarization. Electrophysical measurements have shown that $Si/HfO_2/Ni$ and $Si/HfO_{2(ann)}/Ni$ structures possess ferroelectric properties, the calculated ε of HfO_2 films is 22 and 26, respectively.

Studies have shown that post-growth thermal annealing of hafnium oxide films have a positive effect on capacitive characteristics and reliability of HfO_2-based MDS structures.

Further studies of the $Si/HfO_{2(ann)}/Ni$ structure are planned to investigate the change in maximum and minimum capacitance as a function of the number of switching cycles over 10^6. The results will be presented in future studies.

Funding

This study was supported by grant No. 23-49-10014, provided by the Russian Science Foundation (https://rscf.ru/project/23-49-10014/.).

Conflict of interest

The authors declare that they have no conflict of interest.

References

[1] C.-H. Lee, S.-H. Hur, Y.-C. Shin, J.-H. Choi, D.-G. Park, K. Kim. Appl. Phys. Lett. **86**, 152908 (2005).

[2] D.A. Abdullaev, R.A. Milovanov, R.L. Volkov, N.I. Borgardt, A.N. Lantsev, K.A. Vorotilov, A.S. Sigov. Russ. Technol. J. **8**, *5*, 44 (2020).

[3] T. Mikolajick, S. Slesazeck, H. Mulaosmanovic, M.H. Park, S. Fichtner, P.D. Lomenzo, M. Hoffmann, U. Schroeder. J. Appl. Phys. **129**, 100901 (2021).

[4] R. Guo, Z. Wang, S. Zeng, K. Han, L. Huang, D.G. Schlom, T. Venkatesan, Ariando, J. Chen. Sci. Rep. **5**, 12576 (2015).

[5] E.I. Goldman, D.A. Belorusov, G.V. Chucheva. Ceram. Int. **47**, *15*, 21248 (2021).

[6] D.A. Belorusov, E.I. Goldman, G.V. Chucheva. Physics of the Solid State **64**, *13*, 2140 (2022).

[7] R. Shirota. In: Advances in Non-Volatile Memory and Storage Technology / Ed. Blanka Magyari-Köpe, Yoshio Nishi. Woodhead Publishing, Philadelphia (2019). P. 283.

[8] W. Banerjee, A. Kashir, S. Kamba. Small **18**, *23*, 2107575 (2022).

[9] A. Dkhissi, A. Estéve, C. Mastail, S. Olivier, G. Mazaleyrat, L. Jeloaica, M. Djafari Rouhani. J. Chem. Theor. Comput. **4**, 1915 (2008).

[10] A.P. Huang, Z.C. Yang, P.K. Chu. In: Advances in Solid State Circuits Technologies / Ed. P.K. Chu. In-Tech, Vukovar. (2010). P. 333.

[11] A. Chouprik, A. Chernikova, A. Markeev, V. Mikheev, D. Negrov, M. Spiridonov, S. Zarubin, A. Zenkevich. Microelectron. Eng. **178**, 250 (2017).

[12] E.I. Goldman, A.G. Zhdan, G.V. Chucheva. Instruments and Experimental Techniques **40**, *6*, 841 (1997).

Translated by Y.Alekseev